



Single-mode subwavelength waveguides with wire metamaterials

Pavel A. Belov, Rostyslav Dubrovka, Ivan Iorsh, Ilya Yagupov, and Yuri S. Kivshar

Citation: [Applied Physics Letters](#) **103**, 161103 (2013); doi: 10.1063/1.4824478

View online: <http://dx.doi.org/10.1063/1.4824478>

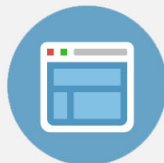
View Table of Contents: <http://scitation.aip.org/content/aip/journal/apl/103/16?ver=pdfcov>

Published by the [AIP Publishing](#)



Re-register for Table of Content Alerts

Create a profile.



Sign up today!



Single-mode subwavelength waveguides with wire metamaterials

Pavel A. Belov,¹ Rostyslav Dubrovka,² Ivan Iorsh,¹ Ilya Yagupov,¹ and Yuri S. Kivshar³

¹National Research University for Information Technology, Mechanics and Optics (ITMO), St. Petersburg 197101, Russia

²Queen Mary University of London, London E1 4NS, United Kingdom

³Nonlinear Physics Center, Research School of Physics and Engineering, Australian National University, Canberra ACT 0200, Australia

(Received 17 July 2013; accepted 23 September 2013; published online 14 October 2013)

We study the guided modes of a slab of wire metamaterial and reveal that such a structure supports deep-subwavelength propagating modes exhibiting the properties of single-mode waveguides at any fixed frequency below the plasma frequency of metal wires. We compare our analytical results with the dispersion relations extracted from the experimental measurements. © 2013 AIP Publishing LLC. [<http://dx.doi.org/10.1063/1.4824478>]

Guided electromagnetic waves are a special type of localized modes which exist either at interfaces of dissimilar media (surface modes) or are trapped by the regions of high-dielectric material (waveguide modes). Guided modes can propagate in various types of waveguides, such as dielectric slab waveguides, photonic fibers, and metallic hollow waveguides.¹ Here we study a type of waveguide created by a slab of wire metamaterial² of a finite thickness, and exhibiting a number of peculiar features not found in conventional waveguides.

Wire metamaterials have a number of unique properties,² including the possibility of the subwavelength image transfer.^{3–5} Localized modes in such structures have been studied theoretically,^{6,7} and it was shown that these modes are similar to the so-called spoof plasmons, a special class of surface modes which propagate along corrugated metal or semiconductor surfaces.^{8–10} It was also shown that these guided modes can be useful for far-field superlensing^{11,12} and deep-subwavelength waveguiding¹³ of electromagnetic waves. However, despite of their peculiar properties, the studies of guided modes and their possible applications were mainly theoretical with no experimental verification of their actual propagation in wire metamaterials.

In this letter, we discuss several unique properties of this type of guided modes, compare them with the corresponding modes of conventional dielectric waveguides, and also present the direct experimental measurements of the guided modes propagation in a slab of wire metamaterial.

We study the waveguiding wire-metamaterial structure shown in Fig. 1(a) where guided modes propagate in the x direction. We describe a slab of wire metamaterial within a local effective theory approach. This approximation is valid when the wire-lattice period is much less than the wavelength. Within this approximation, the wire metamaterial can be characterized by a diagonal tensor of dielectric permittivity $\hat{\epsilon}$ with one component parallel to the wires being equal to infinity, and two other components being equal to the dielectric permittivity $\epsilon = n_m^2$ of the host medium.² Next, we derive the dispersion relations for the waveguide modes of a slab waveguide made of this extremely anisotropic medium [see Fig. 1(b)].

To obtain analytical expressions for the waveguide modes, we consider TM-polarization of light. We then recall that extremely anisotropic metamaterial supports propagation of TEM-polarized waves only with the magnetic field presented by its component $H_y = A \exp(in_mk_0z) + B \exp(-in_mk_0z)$, where k_0 is the wavevector in vacuum. We then apply the continuity boundary conditions for the tangential magnetic and electric fields. Equating the determinant of the obtained linear system to zero, we find the dispersion equation for the localized modes (see also Ref. 14)

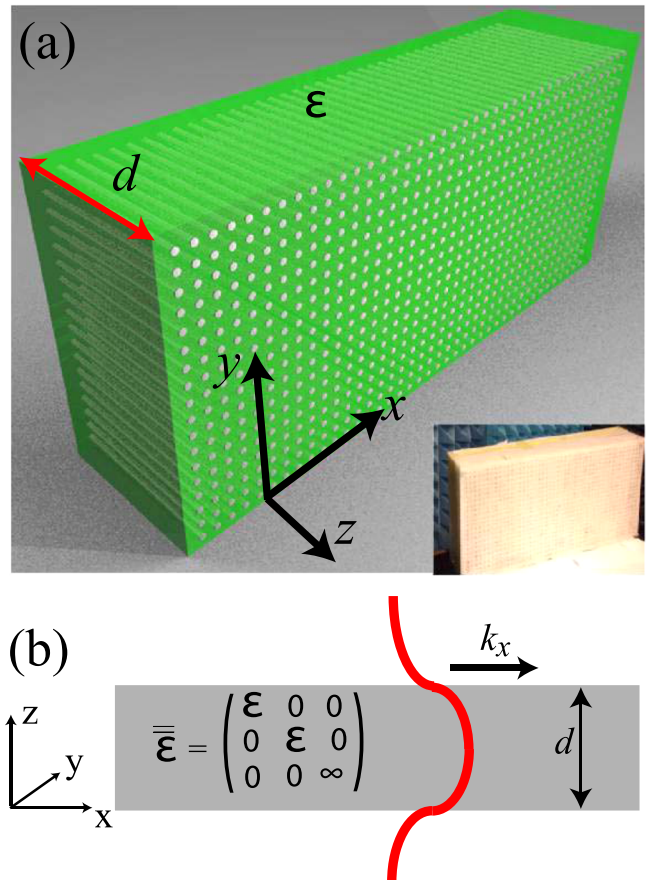


FIG. 1. (a) Geometry of a wire-metamaterial waveguide. Inset shows a photograph of the experimental sample. (b) Propagation of the waveguide mode in the wire-metamaterial slab.

$$k_x = \begin{cases} (k_0/n_m)[\tan^2(n_mk_0d/2) + n_m^2]^{1/2}, & \eta > 0, \\ (k_0/n_m)[\cot^2(n_mk_0d/2) + n_m^2]^{1/2}, & \eta < 0, \end{cases} \quad (1)$$

where $\eta \equiv \tan(n_mk_0d/2)$. When the dielectric host medium is absent ($n_m = 1$), Eq. (1) becomes equivalent to the dispersion relations obtained earlier in Ref. 12.

Figure 2(a) presents the dispersion curves of the guided modes in a wire-metamaterial slab. For comparison, we show also the dispersion curves of the guided modes in a slab of conventional dielectric material of the same thickness with the refractive index $n_m = 2$ [see red and green curves in Fig. 2(a)]. We observe some similarities between the dispersions of dielectric and metamaterial waveguides. In

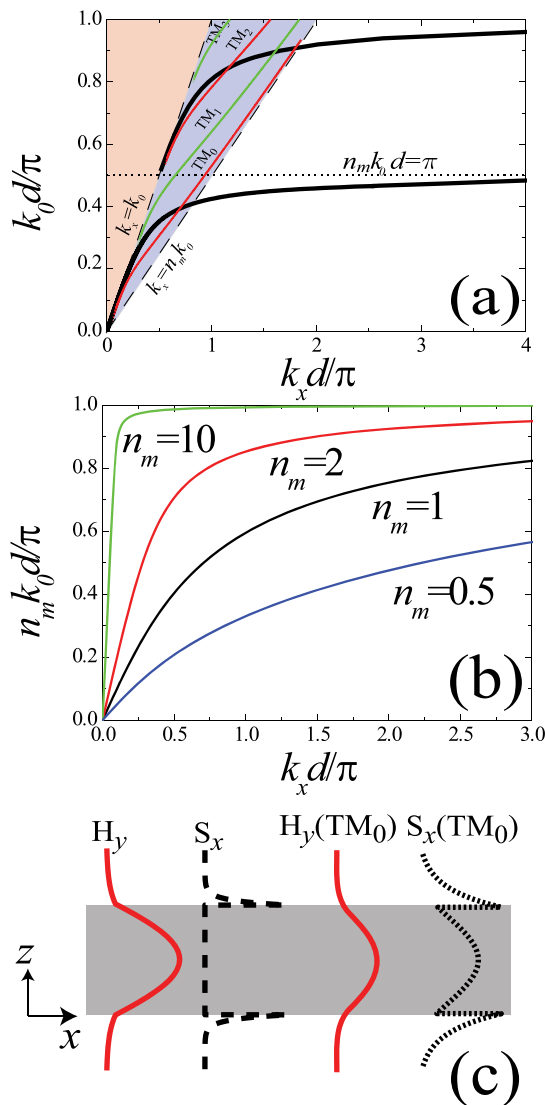


FIG. 2. (a) Dispersion of the guided modes of a wire-metamaterial slab (thick solid curves). Refractive index of the host medium is $n_m = 2$. Pink area shows the region of the propagating modes in free space, blue area shows the region of the existence of the waveguide modes of the corresponding conventional dielectric waveguide with the refractive index $n_m = 2$. Thin red and green lines show the dispersion of the waveguide modes in the dielectric waveguide. (b) Dispersion of the guided modes of a metamaterial slab for different values of refractive index of the host medium. (c) Profile of the magnetic field of the first mode of the wire medium slab. Black dashed line shows the profile of the x component of the Poynting vector, and a black dotted line shows the Poynting vector of the corresponding dielectric waveguide mode.

particular, both structures have only one fundamental eigenmode with no cut-off. Higher-order modes are defined by the cut-off frequencies: $n_mk_0d = \pi n$, for the metamaterial waveguide, and $\sqrt{n_m^2 - 1}k_0d \approx \pi n$, for the dielectric waveguide, where n is the index of the corresponding eigenmode. At the same time, we observe substantial differences between the modes of dielectric and metamaterial waveguides. First, the waveguide number of the dielectric waveguide is always limited with the refractive index of the waveguide core: $k_x < n_mk_0$, thus dispersion curves of all the guided modes lie in the blue area shown in Fig. 2(a). The waveguide number of the eigenmodes in the metamaterial waveguide generally is not bounded provided we do not account for losses and internal periodicity of the metamaterial, and they can extend to infinity, as in the case of surface plasmon polaritons. Moreover, only one eigenmode can exist in the metamaterial waveguide at the fixed frequency, whereas in the case of dielectric waveguide arbitrary large number of modes may exist at the fixed frequency for sufficiently large frequencies. Therefore, the metamaterial slab is a single-mode waveguide for arbitrary frequency (providing that the frequency is below the plasma frequency of metal). We use the term “single-mode” in the same sense as it is used for the planar dielectric waveguides—of course taking into account the possibility of the existence of several modes with different k_y . Thus, our structure as single-mode waveguides in general could benefit from the fact that it can be more effectively coupled to the pump ports and to the antennas.

While the studied eigenmodes exhibit both the properties of guided modes and surface waves, we call them the waveguide modes, because their dispersion depends on the thickness of the metamaterial slab, and the electric field is localized in a bulk rather than at the surface.

Figure 2(b) shows the dispersion curves of the fundamental guided mode of the metamaterial slab depending on the refractive index of the host media. We notice that the guided mode exists even for the case when the refractive index is less than unity, which is not the case for dielectric waveguides, where no guided modes are possible for a low-index core. We should also mention that for the metamaterial eigenmodes the energy is transferred only outside the slab, and no energy transfer is present inside the slab, as shown in Fig. 2(c), since tangential component of the Poynting vector $S_x = \text{Re}[E_z H_y^*]/2$, and E_z component vanishes due to the boundary conditions for the perfectly conducting wires.

Next, we study the waveguide modes experimentally for the microwave frequency range using a sample made of a wire metamaterial shown in Fig. 1. A two-dimensional array of metallic wires of length 10 cm and period of 1 cm is placed in a dielectric host medium. The slab dimensions are $50 \times 25 \times 10$ cm. We excite the metamaterial structure with a point source, positioned at the distance of 3 mm from the structure surface. The signal is then collected with a probe at the opposite side of the structure. Scanning the backside of the structure with the receiver allows to build the amplitude and phase maps of the transmitted radiation.

Figure 3 shows our experimental and numerical results for the transmitted radiation at the frequency 820 MHz, for the case when the source is shifted along the horizontal axis towards the left edge of the structure. In the numerical

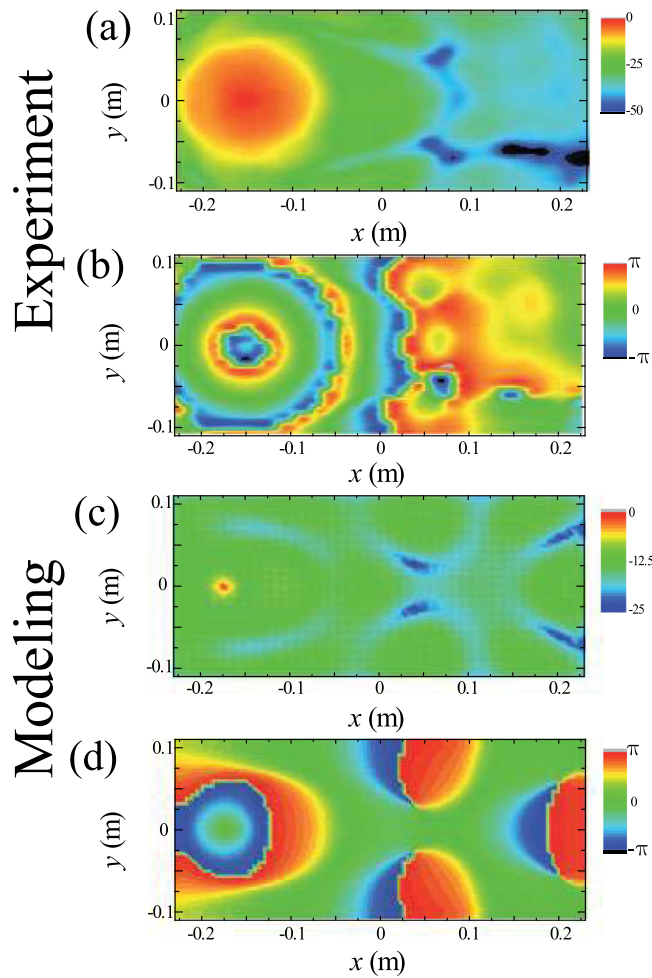


FIG. 3. Experimentally measured (top) and numerically simulated (bottom) (a) and (c) amplitude (in dB) and (b) and (d) phase (in radians) of the transmitted radiation for a source shifted from the center of the device. The frequency is $f = 820$ MHz.

modeling, we observe the excitation of a standing mode formed by surface waves, as predicted earlier.¹² We should mention that in the simulations we have initially undefined parameter which is the refractive index of the host medium (acetal). We have estimated the acetal refractive index as $n_m = 1.56$. In our experiment, the amplitude and phase patterns are significantly blurred, and the presence of a standing wave is hardly distinguishable. This effect could arise due to a number of reasons: first, sensitivity of the experimental measurements is limited significantly by the dynamical range of the setup. In particular, at least 40 dB have been lost due to the source and probe mismatch. The second reason is the presence of losses in the system, which are defined by two mechanisms: inevitable losses in the host medium and the scattering losses of the guided waves by inhomogeneities of the structure interface caused by the slightly different wire length. We note that the latter effect is very frequency-dependent and hardly reproducible in numerical simulations. It is clear that scattering of the guided waves becomes significant when the inhomogeneity characteristic dimension is of the order of the transverse wavelength of the guided wave $\lambda_{\perp} = (2\pi/k_x)$. The minimal characteristic relative size of the inhomogeneity of the wire $\delta d = \Delta d/d$ which is sufficient for the effective scattering of the guided wave decreases as $\cot(n_m k_0 d/2)$ as we are approaching the resonance.

Figure 4 shows the amplitude and phase maps of the transmitted radiation for three different frequencies. The frequencies were chosen such that they cover the area far below the resonance—close to the resonance and blue-shifted from the resonance. We observe a rapid phase change for 860 MHz. Furthermore, the amplitude map of the radiation at this frequency is characterized by a sharp dip at certain distance from the source. It is evident that for smaller and larger frequencies ($f = 760$ MHz and $f = 960$ MHz), none of these distinctive features is observed. Frequency $f = 860$ MHz is close to the analytically obtained resonance value $f_r = 0.959$ GHz which causes a rapid phase change due to a large value of k_x . Moreover, we can notice that the amplitude and phase maps in Figs. 4(c) and 4(d) become blurry when we approach a resonance. We believe that this is due to the shortening of the transverse guided mode wavelength and enhanced scattering on inhomogeneities as discussed above.

Next, we extract the waveguide numbers of the transmitted radiation from the phase maps. Assuming that the most part of the electromagnetic radiation is transferred to guided modes, we take the spatial dependence of the field in the transmitted wave as $E \sim \exp(ik_{\rho}\rho)$, where ρ is the distance from the source in the plane parallel to the structure surface, and k_{ρ} is the wavenumber. Thus, the phase of the transmitted radiation should be linearly proportional to the wavenumber k_{ρ} . Therefore, it is possible to extract the dispersion of k_{ρ} from the phase distribution map measured at different frequencies. Figure 5 shows the extracted values of the wave-number together with the fitting to Eq. (1). We observe that the experimentally obtained dispersion relations agree well with the theoretical results. In the fitting, we use the refractive index of the host medium $n_m = 1.56$.

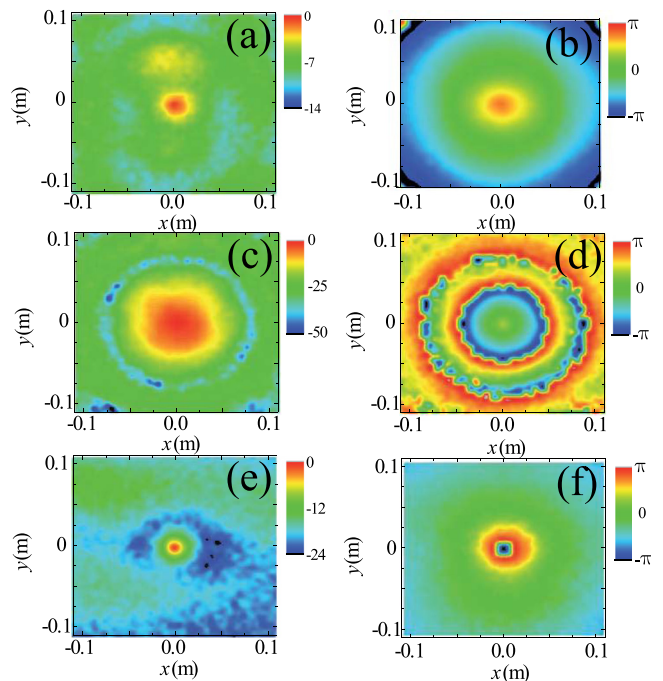


FIG. 4. Experimentally measured amplitude (left column, in dB) and phase (right column, in radians) of the transmitted radiation for different frequencies in the case when the source is placed in the center of the structure for the frequencies: (a) and (b) $f = 760$ MHz, (c) and (d) $f = 860$ MHz, and (e) and (f) $f = 960$ MHz.

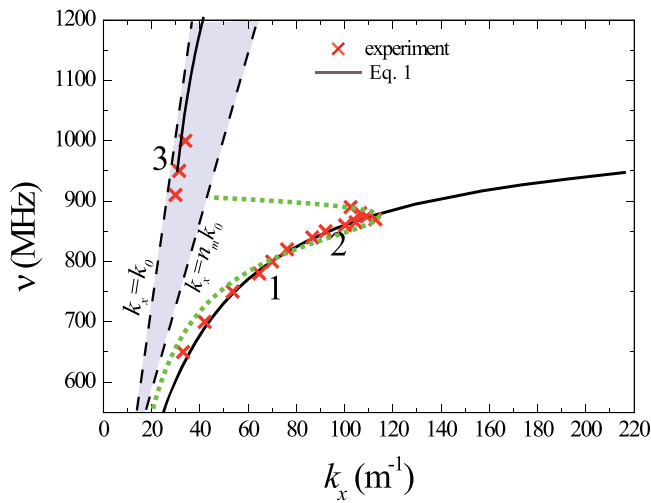


FIG. 5. Dispersion of guided modes extracted from the experimentally measured phase distribution (crosses). Solid curves show the analytical approximation for the dispersion relations for the refractive index $n_m = 1.56$. Blue area shows the domain of existence of the guided modes in the corresponding conventional dielectric waveguide. Green dashed line corresponds to the fitting which takes into account the losses: the refractive index of the host in this case equal to $n_m = 1.55 + 0.054i$.

In Fig. 5 we also observe a bending of the dispersion curve that is typical for the dispersion of surface plasmon polaritons and other surface states in the presence of losses. While we cannot incorporate scattering losses separately into our simple analytical model, we study the effect of losses by adding an imaginary part to the refractive index value in our fitting. Using the least square method we obtain the value of $n_m = 1.55 + 0.054i$ for the dielectric host medium.

In conclusion, we have discussed the properties of waveguiding modes propagating in the slab of wire metamaterial taking into account dielectric permittivity of the host medium,

and compared them with the corresponding properties of conventional waveguides. We have studied experimentally the propagating guided modes in a slab of wire metamaterial and measured their dispersion.

This work was supported by the Ministry of Education and Science of Russian Federation (Grant Nos. 11.G34.31.0020, 14.B37.21.1649, and 14.B37.21.1941), the Dynasty Foundation, Russian Foundation for Basic Research (RFBR 12-02-12097), grant of president of Russian Federation for governmental support of young Russian scientists 6805.2013.2, and the Australian Research Council.

¹A. Yariv, *Optical Electronics* (Holt, Rinehart, and Winston, New York, 1985).

²C. R. Simovsky, P. A. Belov, A. V. Atrashenko, and Y. S. Kivshar, *Adv. Mater.* **24**, 4229 (2012).

³M. G. Silveirinha, P. A. Belov, and C. R. Simovski, *Phys. Rev. B* **75**, 035108 (2007).

⁴P. A. Belov, Y. Zhao, S. Tse, P. Ikonen, M. G. Silveirinha, C. R. Simovski, S. A. Tretyakov, Y. Hao, and C. Parini, *Phys. Rev. B* **77**, 193108 (2008).

⁵P. A. Belov, G. K. Palikaras, Y. Zhao, A. Rahman, C. R. Simovski, Y. Hao, and C. Parini, *Appl. Phys. Lett.* **97**, 191905 (2010).

⁶P. A. Belov and M. G. Silveirinha, *Phys. Rev. E* **73**, 056607 (2006).

⁷Y. Zhao, G. Palikaras, P. A. Belov, R. F. Dubrovka, C. R. Simovski, Y. Hao, and C. G. Parini, *New J. Phys.* **12**, 103045 (2010).

⁸S. A. Maier, S. R. Andrews, L. Martin-Moreno, and F. J. Garcia-Vidal, *Phys. Rev. Lett.* **97**, 176805 (2006).

⁹M. Navarro-Cia, M. Beruete, S. Agrafiotis, F. Falcone, M. Sorolla, and S. A. Maier, *Opt. Express* **17**, 18184 (2009).

¹⁰E. K. Stone and E. Hendry, *Phys. Rev. B* **84**, 035418 (2011).

¹¹F. Lemoult, G. Lerosey, J. Rosny, and M. Fink, *Phys. Rev. Lett.* **104**, 203901 (2010).

¹²F. Lemoult, M. Fink, and G. Lerosey, *Nat. Commun.* **3**, 889 (2012).

¹³F. Lemoult, N. Kaina, M. Fink, and G. Lerosey, *Nat. Phys.* **9**, 55 (2013).

¹⁴F. Lemoult, M. Fink, and G. Lerosey, *Waves Random Complex Media* **21**, 591 (2011).